

DFT AND X-RAY STUDY OF STRUCTURAL, ELECTRONIC, ELASTIC AND OPTICAL PROPERTIES IN $\text{Be}_{1-x}\text{Zn}_x\text{S}$ ALLOYS DEPENDING ON VEGARD'S LAW

A. GULTEKIN^{1,2}, P. PASHAEI^{1,2}, Z. KHAN³, M.K. OZTURK^{1,2}, M. TAMER⁴ & Y. BAS⁵

¹Gazi University Photonic Application and Research Centre, Turkey.

²Physics Department, Science Faculty, Gazi University, Turkey.

³Faculty of Science & Technology, Bournemouth University, UK.

⁴Zirve University, Turkey.

⁵National Boron Research Institute, Turkey.

ABSTRACT

Structural, optical and electronic properties and elastic constants of $\text{Be}_{1-x}\text{Zn}_x\text{S}$ alloys have been studied by employing the commercial code Castep based on density functional theory. The generalized gradient approximation and local density approximation were utilized as exchange correlation. Using elastic constants for compounds, bulk modulus, band gap, Fermi energy and Kramers–Kronig relations, dielectric constants and the refractive index have been found through calculations. Apart from these, X-ray measurements revealed elastic constants and Vegard's law. It is seen that results obtained from theory and experiments are all in agreement.

Keywords: BeZnS, Castep, DFT, Vegard.

1 INTRODUCTION

Semiconductor electrical and optical devices are currently of great demand. II–VI and III–V alloys have been commonly investigated. The use of the compounds beryllium and chalcogens in optoelectronic devices has attracted a great interest. The use of green and blue wavelength within visible region in Leds and Lazer diots is significant [1]. Beryllium chalcogen compounds draw attention owing to BeSe, BeS and BeTe strong lattices, hard and high covalent relations and accordingly, they extend the lifespan of the device [2]. As a result, they were utilized in order to improve the life and hardness of the material [2,3]. Zinc-blend, zinc sulfur (ZnS), zinc tellurium (ZnTe) and zinc tellurium (ZnSe) wide gaps are used in the manufacture of II–VI semiconductors and especially semiconductor devices [4]. It is seen that beryllium chalcogens BeX ($X = \text{S}, \text{Se}, \text{Te}$) that indicate a unique relation between II–VI compounds and large band gaps have recently become focus of interest [5]. Hence, the ternary alloys ($\text{Zn}_{1-x}\text{Be}_x\text{S}$) that Be composes with ZnX are significant in terms of increasing the hardness of material, decreasing the distortion level and extending the life time of an advanced device [6,7].

The other curious property of beryllium chalcogens is the harmony contingency on sublayers in a state of $\text{Zn}_{1-x}\text{Be}_x\text{S}$ ternary alloy [8]. The composition change of $\text{Zn}_{1-x}\text{Be}_x\text{S}$ alloys and bond ionicity lead to substantial alterations on physical properties such as electronic band structures and cage parameters. It is essential to research alloys in detail to advance heterostructures based on these recent material systems. We have studied within AP-LAPW (the full-potential linearized augmented-plane wave) to investigate the structural and electronic properties of alloys composed of beryllium and chalcogens ($\text{Zn}_{1-x}\text{Be}_x\text{S}$) for the design of blue–green laser diots [9]. In this study, we aim to obtain the optical, electronic properties of $\text{Be}_{1-x}\text{Zn}_x\text{S}$ mixed crystals and elastic constants, like bulk modulus, young modulus, shear modulus, Poisson's ratio, compressibility and B/G by means of Castep

program based on density function theory (DFT) and compare the results of the elastic constants obtained via X-ray analyses based on Vegard's law.

2 CALCULATIONS

We obtained the calculations using the plane-wave pseudo-potential method, the commercial CASTEP code [10] based on DFT (Cambridge Sequential Total Energy Package), the generalized gradient approximation (GGA) approach, the norm-conserving Be, Zn and S pseudo-potentials of which were parameterized by Perdew, Burke and Emzerhof and finally the Troullier simulation [11]. That's why, the valence electron configuration for beryllium, zinc and tellurium atom norm-conserving pseudo-potential was used to describe the electron-ion interaction of $2s^2, 3d^{10}4s^2$ versus $5s^25p^4$. In this computer code, plane wave functions of valence electrons were explained through a plane wave base constant and the usage of norm-conserving pseudo-potential allows a plane wave energy E_{cut} . Solely, the kinetic energy which is lower than E_{cut} and plane waves were utilized in expansion. The inter-related space integration upon Brillouin region was similar to a Monkhorst–Pack mesh, which is used by a careful sample in a number ending in k [12]. Wave functions were expanded up to a kinetic energy cut-off of 600 eV value in the state of plane waves. A mesh lattice parameter in Brillouin region, for $x = 0.5$ k-point clusters are $6 \times 6 \times 4$, cut-off value is 350 eV and x other compounds is $4 \times 4 \times 4$ and cut-off value is 620 eV. Charge densities were approximated to 2×10^6 eV/atom using the self-consistent calculations. Energy shift, maximum force, maximum strain and transposition tolerances are received as 2×10^5 eV/atom, 0.05 eV/Å, 0.1 GPa and 0.002 Å. Structural properties of BeS and ZnS binary compounds have been computed within surface-centered cubic structure (F-43M). We have semi-experimentally calculated the structural properties of $A_{1-x}B_xC$ type of ternary alloys within Castep and Vegard's law through X-ray analysis for forces in the position of equilibrium of various $x = 0.25, 0.50, 0.75$ concentrations. Binary and various cut-off values of alloys have been optimized by Castep. Vegard's law elastic constants were experimentally calculated for various $x = 0.25-0.50-0.75$ values using X-ray.

AC and BC are a couple of semiconductors and their semiconductor alloy is $A_{1-x}B_xC$. The compound of x alloy or mole fraction of alloy is the lattice parameter of AC, which is received as a^{AC} , lattice parameter of BC is received as a^{BC} and lattice parameter of alloy is received as $a^{\text{ABC}}(x) = xa^{\text{AC}} + (1-x)a^{\text{BC}}$. This is called Vegard's law [13,14]. Here, while AC is BeS, BC is ZnS. For these components, PDF database numbers (77-2100 and 09-0202) were used and these results were described experimentally with X-ray.

3 RESULTS AND CALCULATIONS

3.1 Electronic and structural properties

There are eight distinct atoms (4 Be and 4 S) within (F-43M) unit cell of surface-centered cubic structure of BeS compound. When we adhere Zn instead of Be, depending on the increased rate of x in $\text{Be}_{1-x}\text{Zn}_x\text{S}_4$ alloy, $\text{Be}_3\text{Zn}_1\text{S}_4$ or $\text{Be}_1\text{Zn}_3\text{S}_4$ is just a simple cubic structure (P-43M) for contingent crystal structure but these are merely a simple tetragonal (P4M2) structure for $\text{Be}_3\text{Zn}_1\text{S}_4$. Bond lengths in $\text{Be}_{1-x}\text{Zn}_x\text{S}_4$ alloy based on the increased x value are shown in Table 1. The maximum value of bond lengths is obtained at $x=0.5$ for Be-S and Be-Zn. S-S and Zn-S bond lengths increase as x rises ($x=0.25, 0.50$ and 0.75).

Table 1: Bond lengths and crystal structures for this study.

$\text{Be}_{1-x}\text{Zn}_x\text{S}$	Space group – construction	Be-S (Å)	Zn-S (Å)	S-S (Å)	Zn-Be (Å)
$\text{Be}_3\text{Zn}_1\text{S}_4$	P-43M cubic	2.14	2.30	3.36	3.55
$\text{Be}_1\text{Zn}_1\text{S}_2$	P-4M2 tetragonal	2.12	2.40	3.39	3.71
$\text{Be}_1\text{Zn}_3\text{S}_4$	P-43M cubic	2.15	2.34	3.51	3.74

Table 2: Band gap, density and lattice parameter values calculated for $\text{Be}_{1-x}\text{Zn}_x\text{S}$.

$\text{Be}_{1-x}\text{Zn}_x\text{S}$	Band gap (eV)	Density (g/cm ³)	Lattice parameter (Å)
BeS	4.17	2.36	4.87
ZnS	1.90	4.09	5.42
$\text{Be}_3\text{Zn}_1\text{S}_4$	3.60	2.79	5.01
$\text{Be}_1\text{Zn}_1\text{S}_2$	3.03	3.22	5.14
$\text{Be}_1\text{Zn}_3\text{S}_4$	2.46	3.65	5.28

By using experimental band gap, density and lattice parameter values for BeS [15] and ZnS [16], and the structural and optical values of $\text{Be}_{1-x}\text{Zn}_x\text{S}$ calculated using Vegard's law are shown in Table 2 for $x=0.25-0.50-0.75$.

We initially computed lattice constants and bulk modulus for each x value of $\text{Be}_{1-x}\text{Zn}_x\text{S}$ via Castep. The experimental and theoretical results are shown in Table 3 [17,18]. Lattice parameters for $\text{Be}_{1-x}\text{Zn}_x\text{S}$ alloys have been explored as 5.02 for $x=0.25$, 4.31–4.31 and 3.63 for $x=0.5$ and 5.35 Å for $x=0.75$, respectively. Lattice parameters appear to be in agreement with those previously calculated [19,20]. The bulk modulus for $\text{Be}_{1-x}\text{Zn}_x\text{S}$ is 88.53–75.38 and 73.72 GPa. The maximum bulk modulus (88.53 GPa) is for $\text{Be}_3\text{Zn}_1\text{S}_4$. Consequently, it is less compressible and its value is 0.016 1/GPa. The compressibility changes according to the increasing value of x ; it is $\text{Be}_3\text{Zn}_1\text{S}_4 < \text{Be}_1\text{Zn}_1\text{S}_2 < \text{Be}_1\text{Zn}_3\text{S}_4$.

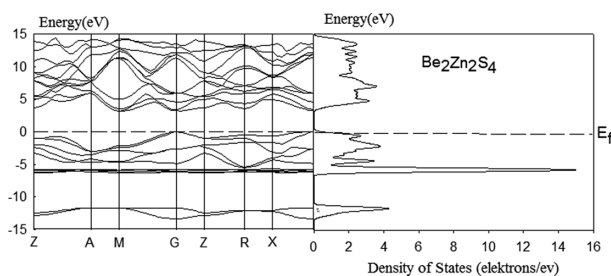
Using lattice constants calculated at equilibrium position for $\text{Be}_{1-x}\text{Zn}_x\text{S}$ alloys; electronic band structures corresponding to high symmetry directions within primary Brillouin region and electronic density of state (DOS) corresponding to band structures have been obtained and indicated in Fig. 1. It is shown that band structures and state densities were in good agreement for all samples but DOS of $\text{Be}_1\text{Zn}_1\text{S}_2$ is given only in Fig. 1. It is seen in band graphic that curves of DOSs create sharp peaks upon bands.

All alloys have a direct band transition and display a semiconductor property. The calculated data and other theoretical data have been listed in Table 4 [9,21]. Band profiles and band gap values are in agreement with the former studies. Band gap energies corresponding to x ($x=0.25, 0.5, 0.75$) of $\text{Be}_{1-x}\text{Zn}_x\text{S}$ alloy are shown in Fig. 1.

Bulk modulus for $\text{Be}_{1-x}\text{Zn}_x\text{S}$ by means of X-ray has been computed as 88.97–85.31–81.71 GPa. The maximum bulk modulus (88.97 GPa) is for $\text{Be}_3\text{Zn}_1\text{S}_4$; it is less compressible and its value is 0.01121/GPa. Compressibility shifts as $\text{Be}_3\text{Zn}_1\text{S}_4 < \text{Be}_1\text{Zn}_1\text{S}_2 < \text{Be}_1\text{Zn}_3\text{S}_4$ according to the increasing x value.

Table 3: Other lattice constant a_0 , bulk modulus, V cell volume experimental and theoretical studies for $\text{Be}_{1-x}\text{Zn}_x\text{S}$.

$\text{Be}_{1-x}\text{Zn}_x\text{S}$	Reference	a_0 (Å)	b_0 (Å)	c_0 (Å)	V (Å) ³	B (GPa)
$\text{Be}_3\text{Zn}_1\text{S}_4$	In this study	5.02	5.02	5.02	127.01	88.53
	In this study (X-ray)	5.01	5.01	5.01	125.75	88.97
	Theory [9] ^a	5.06 ^a	5.06 ^a	5.06 ^a	–	86.60
	Theory [21]	4.98	4.98	4.98	–	92.63
$\text{Be}_1\text{Zn}_1\text{S}_2$	In this study	3.63	3.63	5.35	70.65	75.38
	In this study (X-ray)	5.15	5.15	5.15	136.59	85.31
	Theory [9] ^a	5.21 ^a	5.21 ^a	5.21 ^a	–	80.74
	Theory [21]	5.11	5.11	5.11	–	89.10
$\text{Be}_1\text{Zn}_3\text{S}_4$	In this study	5.30	5.30	5.30	149.02	73.72
	In this study (X-ray)	5.28	5.28	5.28	147.20	81.71
	Theory [9] ^a	5.33 ^a	5.33 ^a	5.33 ^a	–	74.58 ^a
	Theory [21]	5.23	5.23	5.23	–	83.06

Figure 1: $\text{Be}_{1-x}\text{Zn}_x\text{S}$ ($x=50\%$) band structure of Fermi level based on x in 0 and density of state (DOS) have been calculated.Table 4: Other band gap experimental and theoretical studies for $\text{Be}_{1-x}\text{Zn}_x\text{S}$.

$\text{Be}_{1-x}\text{Zn}_x\text{S}$	Reference	E_g (eV)
$\text{Be}_3\text{Zn}_1\text{S}_4$	In this study (Castep)	3.20
	In this study (X-ray)	3.60
	Theory [9]	3.19
	Theory [21]	2.94
$\text{Be}_1\text{Zn}_1\text{S}_2$	In this study	3.18
	In this study (X-ray)	3.03
	Theory [9]	3.22
	Theory [21]	2.95
$\text{Be}_1\text{Zn}_3\text{S}_4$	In this study	2.76
	In this study (X-ray)	2.46
	Theory [9]	2.58
	Theory [21]	2.81

3.2 Elastic properties

The elastic constants of solids establish a relation between mechanical and properties of solids; they provide substantial information about the nature of forces (hardness is related to yield stress) and stability in particular; ab-initio calculation requires a concise method. Forces and elastic constants are related to the first and the second derivatives of the interatomic potentials. The second-order elastic constants are computed within (C_{ij}) ‘Volume-conserving’ technique [22,23]. Six distinct elastic constants are required to be C_{ij} (C_{11} , C_{12} , C_{13} , C_{33} , C_{44} and C_{66}) for a stable tetragonal structure and they need to meet Born–Huang criteria of $C_{11}>0$, $C_{33}>0$, $C_{44}>0$, $C_{66}>0$, $(C_{11}-C_{12})>0$, $(C_{11}+C_{33}-2C_{13})>0$ and $[2(C_{11}+C_{12})+C_{33}+4C_{13}]>0$ in order to maintain stability [17]. Three distinct elastic constants are required to be C_{ij} (C_{11} , C_{12} and C_{44}) for stable cubic crystals [24] and they need to meet Born–Huang criteria of $(C_{11}-C_{12})>0$, $C_{11}>0$, $C_{44}>0$ and $2(C_{11}+C_{12})>0$ in order to maintain stability [17].

We have calculated the elastic constants for $\text{Be}_{1-x}\text{Zn}_x\text{S}$ alloys within Castep and X-ray experimentally. We have obtained six distinct elastic constants for Primitive Tetragonal (P-4M2) structure for $\text{Be}_1\text{Zn}_1\text{S}_2$ when we have computed within Castep. Since we have calculated a primitive cubic (P-43M), we have obtained three distinct elastic constants. Elastic constants we have computed meet all the stability requirements and they are shown in Table 5. It is seen that the results we have computed via both methods are in agreement. We have computed bulk modulus, Young’s modulus, shear (slide) modulus (G), compressibility, B/G ratio and Poisson’s ratio (ν) using elastic constants. We have listed the results in Table 6.

Table 5: Elastic constants we calculated for $\text{Be}_{1-x}\text{Zn}_x\text{S}$ alloys via Castep

$\text{Be}_{1-x}\text{Zn}_x\text{S}$	C_{11}	C_{12}	C_{13}	C_{33}	C_{44}	C_{66}
BeS	155.13 ^a	61.50 ^a			81.6 ^a	
ZnS	104 ^b	65.0 ^c			46.2 ^b	
$\text{Be}_3\text{Zn}_1\text{S}_4$	142.2/143.2	62.33	–	–	72.79/70.59	–
$\text{Be}_1\text{Zn}_1\text{S}_2$	129.5/112.9	63.25	–/55.13	–/112.76	63.93/68.91	–/61.70
$\text{Be}_1\text{Zn}_3\text{S}_4$	116.8/108.7	63.25	–	–	55.0655.5	–

^{a,b}References [4,25].

Table 6: Results we calculated via Castep for bulk modulus (B), Young’s modulus (E), shear modulus (G), compressibility, B/G, Kleinman parameter (ξ) and Poisson’s ratio (ν) for $\text{Be}_{1-x}\text{Zn}_x\text{S}$ alloys.

$\text{Be}_{1-x}\text{Zn}_x\text{S}$	Poisson ratio (ν)	Bulk modulus (B)	Shear modulus (G)	B/G	Compressibility (1/GPa)	Kleinman parameter (ξ)
$\text{Be}_3\text{Zn}_1\text{S}_4$	0.29/0.30	88.53/88.97	61.10/57.22	1.38/1.49	0.0112/0.0112	0.56/0.57
$\text{Be}_1\text{Zn}_1\text{S}_2$	0.32/0.32	75.38/85.31	46.99/49.11	1.60/1.65	0.0132/0.0117	0.64/0.61
$\text{Be}_1\text{Zn}_3\text{S}_4$	0.34/0.35	73.72/81.06	41.10/41.21	1.68/1.85	0.0135/0.0123	0.63/0.65

Bulk modulus, Young's modulus, shear (slide) modulus (G), compressibility, B/G ratio and Poisson's ratio (ν) can be correlated indirectly to brittleness [19]. $B/G > 1.75$ means that the alloy is flexible; $B/G < 1.75$ means that the alloy is brittle [20]. The alloy and bulk modulus (B) of which is larger is less compressible. Poisson's ratio ν value is lower than 0.1 for covalent materials. The typical ν value of ionic materials is 0.25 [26]. Poisson's ratio of a material can act flexibly for $\nu > 1/3$ and it can act in a brittle way for $\nu < 1/3$ [27]. Poisson's ratio values of (ν)=0.25 and (ν)=0.5 are the upper and lower limit of the force fields within the center of solids [28]. Kleinman parameter ξ defined as internal strain is an important parameter [29] and is related to maximum strains. If $\xi=0$, atom remains in the center on distorted four-faced. If $\xi=1$, bond twist appears [30].

3.3 Debye temperature

Debye temperature is the temperature of the crystal's highest vibration mode, and is shown with θ_D . Moreover, it is a fundamental physical characteristic about elastic constant and melting point. It is used to classify the solids according to their high and low temperature zones. Let the temperature be T, if Debye temperature is $T > \theta_D$, it shows that all modes have $k \beta_T$ energy, however, if $T < \theta_D$, it shows high-frequency modes are frozen [30]. It is concluded that phonon vibrational wavelengths are small on Debye temperature; if it is below, it is big. The calculation of Debye temperature can be found in Reference [31].

Average value of speed of sound is calculated from the following equation:

$$v_m = \left[\frac{1}{3} \left(\frac{2}{v_l^3} + \frac{1}{v_t^3} \right) \right]^{-1/3} \quad (1)$$

v_l and v_t are longitudinal and transverse wave speed, respectively. From Navier equation [32],

$$v_l = \sqrt{\frac{3B + 4G}{3\rho}} \quad \text{and} \quad v_t = \sqrt{\frac{G}{\rho}} \quad (2)$$

are obtained. Here G is the shear module. For $\text{Be}_{1-x}\text{Zn}_x\text{S}$, density (ρ) is listed in Table 7 by calculating the longitudinal (v_l), transverse (v_t) and (v_m) speed of sound and Debye temperature with Castep and X-ray.

Table 7: Density (ρ), longitudinal (v_l), transverse (v_t), average (v_m) elastic wave velocities and Debye temperature (θ_D) for $\text{Be}_{1-x}\text{Zn}_x\text{S}$ in this study.

$\text{Be}_{1-x}\text{Zn}_x\text{S}$	ρ (g/cm ³)	v_l (10 ³ m/s)	v_t (10 ³ m/s)	v_m (10 ³ m/s)	θ_D (K)
$\text{Be}_3\text{Zn}_1\text{S}_4$ (Castep)	2.92	4.74	7.63	5.06	525
$\text{Be}_3\text{Zn}_1\text{S}_4$ (X-ray)	2.79	4.53	7.70	5.02	513
$\text{Be}_2\text{Zn}_2\text{S}_4$ Castep)	3.25	3.80	6.52	4.22	482
$\text{Be}_2\text{Zn}_2\text{S}_4$ (X-ray)	3.22	3.90	6.84	4.34	494
$\text{Be}_1\text{Zn}_3\text{S}_4$ Castep)	3.78	3.30	5.83	3.67	475
$\text{Be}_1\text{Zn}_3\text{S}_4$ (X-ray)	3.66	3.35	6.09	3.74	479

3.4 Optical properties

When the electromagnetic radiation is sent upon the material, optical phenomena start as a consequence of the interaction of photons and electron atoms. If the dispatched photons have an energy which is equal to the banned energy gap (E_g), the electron of the material is stimulated to high-energy level. If their energy is lower than the energy gap, photons are replaced instead of absorption and the material is defined as lucid [33].

In this work, we need to define the linear reaction of dielectric function to electromagnetic radiation about the interaction of photons of $\epsilon(\omega)$ with electrons in order to investigate the optic behavior of $\text{Be}_{1-x}\text{Zn}_x\text{S}$. $\epsilon_2(\omega)$, which is known as the imaginary part of dielectric function, can be calculated through the matrix components of momentum and the selection rule of filled and unfilled wave functions. The real part of the dielectric function $\epsilon_1(\omega)$ is related to Kramers–Kronig relation. Other optical properties were derived from the complex part of the dielectric function. Definitions to describe dielectric functions, refractive index $n(\omega)$ and extinction coefficient $K(\omega)$ can be found in Refs. [34,35]. Results are listed in Fig. 2.

There is a relation between refraction subscript in low frequencies and dielectric constant shown below:

$$n(0) = \epsilon^{1/2}(0). \quad (3)$$

Refraction subscript and dielectric constants are important in determining the optic and electric feature of crystal. A few experiments interrelate band gap and refraction of semiconductors. This experimental relation is taken from Refs. [36,37]

$$n = \sqrt{1 + \left(\frac{A}{E_g + B} \right)^2} \quad (4)$$

Here $A=13.6$ eV and $B=3.4$ eV. With this method, dielectric constant and refraction subscript which were obtained experimentally by X-ray and theoretically by Castep for this compound are compared in Table 8.

The fundamental peaks of real part of dielectric function is 5.69–7.11–6.20 eV for contribution values of $x=0.25$ – 0.50 – 0.75 , respectively. The frequency value of $\epsilon_1(0)=5.38$ – 5.85 – 5.66 eV gives the static dielectric constant for $x=0.25$ – 0.50 – 0.75 , respectively. The imaginary part of dielectric constant commences to absorb the radiation around 3.23–3.19–2.8 eV according

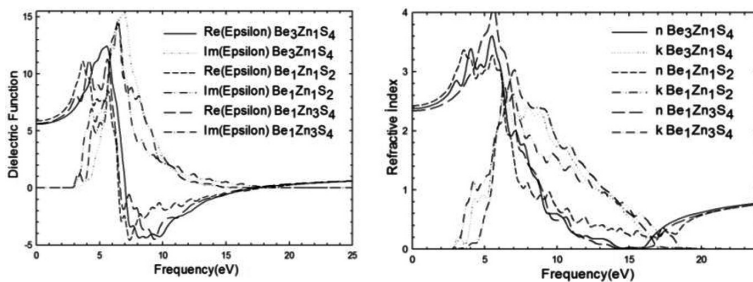


Figure 2: (a) Real and imaginary parts of dielectric constant and (b) refraction (n) constant and extinction (k) constant.

Table 8: Refractive index n and the real part of dielectric function for $\text{Be}_{1-x}\text{Zn}_x\text{S}$.

$\text{Be}_{1-x}\text{Zn}_x\text{S}$	$n(0)$	$\epsilon(0)$	E_g (eV)
$\text{Be}_{0.75}\text{Zn}_{0.25}\text{S}$ (Castep)	2.32	5.38	3.20
$\text{Be}_{0.75}\text{Zn}_{0.25}\text{S}$ (X-ray)	2.25	5.06	3.60
$\text{Be}_{0.5}\text{Zn}_{0.5}\text{S}$ (Castep)	2.42	5.85	3.18
$\text{Be}_{0.5}\text{Zn}_{0.5}\text{S}$ (X-ray)	2.36	5.57	3.03
$\text{Be}_{0.25}\text{Zn}_{0.75}\text{S}$ (Castep)	2.38	5.66	2.76
$\text{Be}_{0.25}\text{Zn}_{0.75}\text{S}$ (X-ray)	2.49	6.20	2.46

to the contribution values. These are close to band gap energy, represent the optical transition between conductivity band and the valence band. Alloy acts as a brittle substance until the value in which the dispersion curve begins to increase and this is the region that dispersion is minor. Values when the imaginary part of dielectric constant is maximum are 6.82–3.84–5.4 eV for contribution values of $x=0.25$ – 0.50 – 0.75 , respectively. These values correspond to interband transitions [38].

4 CONCLUSIONS

In this study structural, electronic, optical properties and elastic constants for $\text{Be}_{1-x}\text{Zn}_x\text{S}$ have been investigated within the commercial code Castep based on DFT. The GGA has been used for the exchange correlation. Using Castep program and X-ray device, elastic constants for zero pressure have been calculated and based on elastic constants, bulk modulus (B), Young's modulus (E), Shear modulus (G), compressibility, B/G and Poisson's ratio (ν) have been calculated. The results we computed by means of both methods are as follows:

1. Since B/G ratio of $\text{Be}_1\text{Zn}_3\text{Te}_4$ alloy obtained through X-ray and Castep is larger than 1.75; other flexible alloys have brittle property.
2. Since Poisson's ratio (ν) values are larger than 0.25, they have an ionic property.
3. Since Poisson's ratio (ν) is between 0.25 and 0.5, interatomic forces are central in these compounds.
4. If Poisson's ratio is $\nu > 1/3$, the material act flexibly; if $\nu < 1/3$; then the material acts in a brittle way. According to this information, $\text{Be}_1\text{Zn}_3\text{S}_4$ other flexible alloys demonstrate a brittle property within both methods.
5. The calculated results show that all alloys have a direct band transition and semiconductor property.

ACKNOWLEDGMENT

The authors acknowledge that this work was supported by the Ministry of Development of TR under Project No. 2011K120290.

REFERENCES

- [1] Gunshor, R. & Nurmikko, A., *Mater. Res. Bull.*, **20**, p. 15, 1995.
- [2] Verie, C., *J. Cryst. Growth*, **1061**, pp. 184–185, 1998.
- [3] Maruyama, K., Suto, K. & Nishizawa, J.-I., *J. Cryst. Growth*, **104**, pp. 214–215, 2000.

- [4] Wang, H.Y., Cao, J., Huang, X.Y. & Huang, J.M., *Condens Matter Physics*, **15(1)**, 13705, pp. 1–10, 2012.
- [5] Kuskovsky, I.L., Gu, Y., Vander Voort, M., Tian, C., Kim, B., Herman, I.P., Neumark, G.F., Guo, S.P., Maksimov, O. & Tamargo, M.C., *Phys. Stat. Sol. (b)*, **229(1)**, p. 239, 2002. doi: [http://dx.doi.org/10.1002/1521-3951\(200201\)229:1%3C239::AID-PSSB239%3E3.0.CO;2-G](http://dx.doi.org/10.1002/1521-3951(200201)229:1%3C239::AID-PSSB239%3E3.0.CO;2-G)
- [6] Kuskovsky, I., Tian, C., Sudbrack, C., Neumark, G.F., Guo, S.P. & Tamargo, M.C., *J. Cryst. Growth*, **214**, pp. 335–339, 2000. doi: [http://dx.doi.org/10.1016/S0022-0248\(00\)00108-1](http://dx.doi.org/10.1016/S0022-0248(00)00108-1)
- [7] Buchley, M.R., Peiris, F.C., Maksimov, O., Muñoz, M. & Tamargo, M.C., *Appl. Phys. Lett.*, **81**, p. 5156, 2002. doi: <http://dx.doi.org/10.1063/1.1534387>
- [8] Faurie, J.P., Bousquet, V., Brunet, P. & Tournie, E., *J. Cryst. Growth*, **184**, p. 11, 1998. doi: [http://dx.doi.org/10.1016/S0022-0248\(98\)80284-4](http://dx.doi.org/10.1016/S0022-0248(98)80284-4)
- [9] Baaziz, H., Charifi, Z., El Haj Hassan, F., Hashemifar, S.J. & Akbarzadeh, H., *Phys. Stat. Sol. (b)*, **243(6)**, p. 1296, 2006. doi: <http://dx.doi.org/10.1002/pssb.200541481>
- [10] Segall, M.D., Lindan, P.J.D., Probert, M.J., Pickard, C.J., Hasnip, P.J., Clark, S.J. & Payne, M.C., *J. Phys. Condens. Matter*, **14(11)**, p. 2717, 2002. doi: <http://dx.doi.org/10.1088/0953-8984/14/11/301>
- [11] Fischer, T.H. & Almlöf, J., *J. Phys. Chem.*, **96**, p. 9768, 1992. doi: <http://dx.doi.org/10.1021/j100203a036>
- [12] Monkhorst, H.J. & Pack, J.D., *Phys. Rev. B*, **13(12)**, p. 5188, 1976.
- [13] Androulidaki, M., Pelekanos, N.T., Tsagaraki, K., Dimakis, E. & Iliopoulos, E., **b3(6)**, p. 1866, 2006.
- [14] Wu, J., Walukiewicz, W., Yu, K.M., Ager, III J.W., Li, S.X., Haller, E.E., Hai, Lu. & Schaff, W.J., *Solid State Commun.*, **127**, p. 411, 2003. doi: [http://dx.doi.org/10.1016/S0038-1098\(03\)00457-5](http://dx.doi.org/10.1016/S0038-1098(03)00457-5)
- [15] Narayana, C., Nesamony, V.J. & Ruoff, A.L., *Phys. Rev. B*, **56**, p. 14338, 1997. doi: <http://dx.doi.org/10.1103/PhysRevB.56.14338>
- [16] Okuyama, H., Kishita, Y. & Ishibashi, A., *Phys. Rev. B.*, **57**, p. 2257, 1998.
- [17] Born, M. & Huang, K., *Dynamical Theory of Crystal Lattices*, Clarendon: Oxford, 1956.
- [18] Zhai, H., Li, X. & Du, J., *Mater. Trans.*, **53(7)**, p. 1247, 2012.
- [19] Matori, K.A., Zaid, M.H.M., Sidek, H.A.A., Halimah, M.K., Wahab, Z.A. & Sabri, M.G.M., *Int. J. Phys. Sci.*, **5(14)**, p. 2212, 2010.
- [20] Ponomareva, A.V., Isaev, E.I., Vekilov, Yu.Kh. & Abrikosov, I.A., *Phys. Rev. B*, **85**, p. 144117, 2012.
- [21] Ameri, M., Rached, D., Rabah, M., El Haj Hassan, F., Khenata, R. & Doui-Aici, M., *Phys. Stat. Sol. (b)*, **245(1)**, p. 106, 2008.
- [22] Ashcroft, N.W. & Mermin, N.D., *Solid State Physics*, Saunders College: Philadelphia, PA, 1976.
- [23] Nye, J.F., *Physical Properties of Crystals*, Clarendon: Oxford, 1957.
- [24] Wu, Z.-J., Zhao, E.-J., Xiang, H.-P., Hao, X.-F., Liu, X.-J. & Meng, J., *Phys. Rev. B*, **76**, p. 054115, 2007.
- [25] Jing, C., Xiang-Rong, C., Wei, Z. & Jun, Z., *Chin. Phys. Soc.*, **17(4)**, p. 1674, 2008.
- [26] Bannikov, V.V., Shein, I.R. & Ivanovskii, A.L., *Phys. Status Solidi. Rapid Res. Lett.*, **3**, p. 89, 2007.
- [27] Frantsevich, I.N., Voronov, F.F. & Bokuta, S.A., *Elastic Constants and Elastic Moduli of Metals and Insulators Handbook*, ed. I.N. Frantsevich, Naukova Dumka: Kiev, 1983.

- [28] Shena, Y. & Zhou, Z., *J. Appl. Phys.*, **103**, p. 074113, 2008.
- [29] Kleinman, L., *Phys. Rev.*, **128(6)**, p. 2614, 1962.
- [30] Firszt, F., Legowski, S., Meczyiska, H. & Szatkowski, J., *Acta Phys. Pol. A*, **88(4)**, 1995.
- [31] Chrisman, J.R., *Fundamentals of Solid State Physics*, John Wiley: New York, pp. 217–218, 1988.
- [32] Johnston, I., Keeler, G., Rollins, R. & Spicklemire, S., *Solid State Physics Simulations*, The Consortium for Upper-Level Physics Software, John Wiley: New York, pp. 45–59, 1996.
- [33] Fox, M., *Optical Properties of Solids*, Oxford Master Series in Condensed Matter Physics, Oxford University Press: Oxford, 2001.
- [34] Dadsetani, M. & Pourghazi, A., *Phys. Rev. B*, **73**, p. 195102, 2006.
- [35] Wooten, F., *Optical Properties of Solids*, Academic: New York, 1972.
- [36] Herve, J.P.L. & Vandamme, L.K.J., *Infrared Phys. Technol.*, **35**, 609, 1994. doi: [http://dx.doi.org/10.1016/1350-4495\(94\)90026-4](http://dx.doi.org/10.1016/1350-4495(94)90026-4)
- [37] Hosseini, S.M., *Phys. B Condensed Matter*, **403(10-11)**, p. 1907, 2008. doi: <http://dx.doi.org/10.1016/j.physb.2007.10.370>
- [38] Khenata, R., Bouhemadou, A., Sahnoun, M., Reshak, A.H., Baltache, H., & Rabah, M., *Comput. Mater. Sci.*, **38(1)**, pp. 29–38, 2006. doi: <http://dx.doi.org/10.1016/j.commatsci.2006.01.013>